Efficient degradation of selected polluting dyes using the tetrahydroxoargentate ion, Ag(OH)$_4^-$, in alkaline media

Ileana R. Zamora-Garcia [a], Alejandro Alatorre-Ordaz [a, *], Jorge G. Ibanez [b],
Julio C. Torres-Elguera [a], Kazimierz Wrobel [a], Silvia Gutierrez-Granados [a]

[a] Departamento de Quimica, Unidad Pueblito de Rocha, Campus Guanajuato, Universidad de Guanajuato, Cerro de la Venada s/n, Col. Pueblito de Rocha, CP 36040, Guanajuato, Mexico
[b] Depto. de Ing. y Ciencias Quimicas, Centro Mexicano de Quimica Verde y Microescala, Universidad Iberoamericana-Ciudad de Mexico, Prol. Reforma 880, 01219, Mexico City, Mexico

HIGHLIGHTS

- We applied the reported tetrahydroxoargentate ion Ag(OH)$_4^-$ for oxidation of surrogate organic recalcitrant dyes, by indirect redox oxidation.
- Through UV-Vis and chromatography techniques, we showed the possibility to degrade recalcitrant compounds such as fluorescein and rhodamine.
- Possible mechanisms of this indirect oxidation dye process using Ag(OH)$_4^-$ are suggested.

ARTICLE INFO

ABSTRACT

The use of soluble and highly oxidizing Ag(III) in the form of the tetrahydroxoargentate ion Ag(OH)$_4^-$ is reported for the oxidation of surrogate organic recalcitrant dyes (i.e., rhodamine 6G (Rh6G) and fluorescein (Fl)). The possible use of Ag(OH)$_4^-$ for the treatment of these and other refractory compounds is assessed. Such dyes were selected due to their common occurrence, stability, refractory nature, the relatively high toxicity of Rh6G, and their structural similarity to Fl. Several reaction intermediates/products were identified. The results showed that the highly oxidizing tetrahydroxoargentate anion was capable of degrading these recalcitrant dyes. Furthermore, the final degradation products do not represent a higher environmental risk than the original surrogates themselves. In addition, the partial mineralization of the dyes was proven.

1. Introduction

Textile industries often release large volumes of problematic wastewaters associated with intense coloration and adverse effects on human health (Farida et al., 2009). More than 10^5 dyes are available today; the industrial use of these dyes generates over 7×10^5 tons of dyes in wastewaters worldwide (Wu and Jane, 2003), particularly from the textile, paper, food, cosmetic, and pharmaceutical industries (Natarajan et al., 2011). Their elimination has prompted the use of new technologies. The most common physicochemical remediation methods include membrane filtration, coagulation, flocculation, oxidation and photoprocesses (such as UV, Fenton, H_2O_2 and O_3 oxidation), and adsorption (Farida et al., 2009; Natarajan et al., 2011; Yu et al., 2009; Peralta et al., 2008; He et al., 2009a,b; Li et al., 2007). Ozonation is particularly suited for this undertaking, but it is expensive. Membrane filtration, coagulation, flocculation and adsorption can remove color, but they are typically associated with bulky sludge production and intense requirements for added chemicals.

The photocatalytic approach using UV-irradiated semiconductor suspensions offers high chemical stability, high catalytic activity, and relatively low toxicity and cost (Natarajan et al., 2011; Yu et al.,

---

* Corresponding author.
  E-mail address: alatorre@ugto.mx (A. Alatorre-Ordaz).

2009; He et al., 2009a,b; Li et al., 2007). Unfortunately, most photocatalysts are active only in the UV region (Li et al., 2007). $NaBiO_3$, Bi_2WO_6, and Bi_2O_6 extend the usable sunlight wavelength range, but their photoactivity is relatively low, with concomitant slow degradation rates (Yu et al., 2009; He et al., 2009a,b; Li et al., 2007).

Electrochemical methods offer promising alternatives. In this context, Ag(III) can be explored as a possible redox mediator in its soluble form, which is the tetrahydroxoargentate anion $Ag(OH)_4^-$ in alkaline media (Cohen and Atkinson, 1968). Its notably high standard potential (1.8 V vs. NHE) makes it attractive for the treatment of many organic compounds. We have previously reported its preparation by electrolysis from metallic silver in alkaline solutions and its characterization (Zamora-Garcia et al., 2013). The usage of the tetrahydroxoargentate ion has not been reported for the transformation of recalcitrant organic species in water.

In the present work, we report the indirect electrodegradation with $Ag(OH)_4^-$ of two types of dyes as pollutant models: rhodamine (Rh6G) and fluorescein (Fl). Rh6G has a rigid structure, extraordinary photostability, and a bio-refractory nature (Yu et al., 2009; Li et al., 2009; Zheng et al., 2012; He et al., 2009a,b; Fu et al., 2005), but low solubility in alkaline media. Conversely, Fl exhibits a similar structure and properties but with high solubility in such media.

Rhodamines and their derivatives contain fluorophores and chromophores that have attracted considerable attention due to specific photophysical properties, such as high molar extinction coefficients (e.g., that for Rhodamine 6G is 116,000 M^{-1} cm^{-1}) (Farida et al., 2009), which allow their use in dye-lasers, molecular imaging, and selective ion chemosensing (He et al., 2009a,b; Fang-Jun et al., 2010). A highly sensitive, rhodamine-based colorimetric off-on fluorescent chemosensor has been developed for Hg^{2+} in aqueous solution and for live cell imaging (Wang et al., 2011; Hochberger et al., 1998). Rh6G is a very soluble cationic dye (Zheng et al., 2012) that is typically used as a dye for paper and for natural (e.g., silk, cotton, wool, leather, bast fibers) and synthetic fibers, as well as a water pollution tracer, an absorption indicator, and in personal care and cosmetic products. Criminologists use it for latent printing and identification purposes (Masters, 1990).

Since most synthetic dyes pose environmental risks to some degree, we selected Rh6G as a model pollutant considering that its rigid closed ring structure contributes to its stability and bio-refractivity (Zheng et al., 2012; He et al., 2009a,b; Farida et al., 2009; Yu et al., 2009; Fu et al., 2005), and its relative toxicity. For example, Rh6G is a potent inhibitor of oxidative phosphorylation (Gear, 1974); rat mortality after Rh6G injection is well documented (French, 1989) as well as its toxic effect on rat retinal ganglion cells (Thaler et al., 2008).

Even though its toxicity is generally regarded as low (TOXNET, 2017), the yellow dye fluorescein was also selected for the present study due to its structural similarity with Rh6G and to its much higher solubility in alkaline media. Fluorescein is used in many applications: as a presumptive reagent for dilute blood detection; in cosmetics, cleansers, and other household products; as a tracer for water leaks and water pollution sources; as an adsorption indicator; as a chemical intermediate for other dyes; and as a fluorescent pH indicator (Lide, 2007). Its sodium salt has several uses in ophthalmology (Dolak et al., 2008).

In the present work, UV—Vis spectrophotometry, total organic carbon (TOC), and high-pressure liquid chromatography (HPLC) were used to identify the species involved at different reaction stages and to evaluate the degree of mineralization. Gas chromatography with flame ionization detection (GC-FID) was used as a qualitative way to monitor the rupture and degradation of the dyes. Lastly, gas chromatography with mass spectrometry (GC-MS) detection was used to identify the final reaction products.

2. Materials and methods

2.1. Preparation of $Ag(OH)_4^-$

A conventional three-electrode cell was used with a silver mesh ($0.15 \times 10 \times 10$ mm, 99.99%, NILACO) as the working electrode, a 5-cm-long, $\Phi = 0.7$ mm Pt wire as the counter electrode (Sigma-Aldrich, USA), and a Ag/AgCl reference electrode (Bioanalytical systems, USA). The Ag mesh was prewashed with 10% HNO_3 (prepared from 70% HNO_3, Karal) to eliminate its natural passivation layer. The supporting electrolyte was 4.0 M NaOH (Karal, 97%). Milli-Q water was used at room temperature throughout the entire experimental procedure. Potentials were applied with a PAR 273A potentiostat (Princeton Applied Research, USA). $Ag(OH)_4^-$ was electrogenerated by applying a constant potential of 1.2 V to this cell for 10 min, which produced a 0.113 mmol/L solution (Zamora-Garcia et al., 2013).

2.2. UV—Vis spectrophotometry

In a 2-mL Eppendorf tube, 1 mL of the $Ag(OH)_4^-$ solution described above was mixed with either an aliquot from an 880-ppm Rh6G stock solution (prepared with 100 mL of Milli-Q water and 0.088 g of Rh6G, Sigma, 98%) or with an aliquot from an 800-ppm Fl stock solution (prepared with 100 mL of 4.0 M NaOH and 0.080 g of Fl, Wako, 98%), to generate a 40-ppm solution of dye in each case. Wavelength scans from 250 to 800 nm were performed with an AVA Spec 048 spectrophotometer (Avantes, The Netherlands). Reaction times varied up to 120 min; the dye-to-oxidant ratios were 1:18 Rh6G:$Ag(OH)_4^-$ and 1:9 Fl:$Ag(OH)_4^-$, and the pH was ca. 16 in all cases.

2.3. TOC measurements

A 1110-ppm Fl stock solution (dissolved in 4.0 M NaOH) and a 500-ppm Rh6G solution (dissolved in water) were used. Aliquots of these dye stock solutions were used to generate 10—50 ppm solutions for the ensuing experiments. The TOC content of the stock solutions was measured at different dilutions with a Shimadzu TOC-V$_{CPH}$ instrument (Japan), which required 15 mL of sample for every determination. Prior to injection into the TOC apparatus, samples were acidified to pH $\leq$ 3 with HCl (J.T. Baker, 75%), purged with bubbling air to eliminate the CO_2 produced in this acidification step, and centrifuged to separate any remaining solid particles.

2.4. Sample preparation for the chromatographic characterization

These samples also required acidification to 1 < pH < 3 with HCl (J.T. Baker, 75%) prior to injection into the different chromatographic analytical systems. The procedure also involved the following: a) salting out with NaCl (Karal, 99%) to saturate the aqueous phase and make the extraction more efficient, b) three successive extractions with CH_2Cl_2 (J.T. Baker, 99.5%) to recover the highest possible amount of analytes, c) solvent evaporation with air, and d) redissolution in CH_3OH (Karal, 99.5%), $C_6H_5CH_3$ (Karal, 99.5%), or CH_3CN (Karal, 99.5%), as needed.

2.5. HPLC

Reversed-phase chromatography was performed with a PM-80 BAS chromatograph using a C_{18}, 15 cm $\times$ 4.6 mm column (Supelco, 5 μm). For the detection of possible N-de-ethylated intermediates generated during the degradation of dyes (He et al., 2009a, 2009b), a 45% ammonium acetate (13 mM) and 55% methanol solution was used as the mobile phase. Samples were analyzed

at 250 and 450 nm with a UV-116A BAS UV–Vis detector. To determine organic acids, extractions were performed with ethyl acetate, and the detection was set at 210 and 230 nm. The mobile phase was 0.1% H_3PO_4 (Sigma, HPLC grade 98%, solution A) with acetonitrile (Sigma-Aldrich HPLC grade 99.9%, solution B) using the following elution gradients: t = 0 min, 100% A and 0% B; t = 15 min, 80% A and 20% B; t = 24 min, 60% A and 40% B; and t = 35 min, 50% A and 50% B (Lei and Dai, 2007).

2.6. GC-MS

To select the dye:Ag(OH)$_4^-$ molar ratio allowing us to observe the largest number of peaks for the best dye degradation, which was key information for subsequent GC-MS analyses, gas chromatography with flame ionization detection (GC-FID) analyses were performed (not shown here). Once the necessary molar ratio was determined, GC-MS analyses were used for identification purposes. For Rh6G, the 1:18 Rh6G:Ag(OH)$_4^-$ molar ratio gave the largest number of peaks, whereas the best molar ratio for the Fl:Ag(OH)$_4^-$ system was 1:9.

A Bruker 456 gas chromatograph (USA), coupled to a Scion TQ mass spectrometer (USA), was used with a Bruker BR-5 MS column (15 m, Φ = 0.25 mm, 0.25 μm film thickness) for the GC-MS analyses. The electron-impact ionization energy was 70 eV, and the full scan mode was selected from 80 to 500 m/z. The injection port was split 10:1 at a temperature of 250 °C, with high purity He as the carrier gas at a flow of 1.0 mL min^{-1}. The oven program was as follows: 80 °C initial temperature, holding for 1 min, then ramping to 260 °C at 10 °C min^{-1}, and then holding for 1 min. The temperature values for the transfer-line heater and ion source of the mass spectrometer were 250 °C and 200 °C, respectively.

3. Results and Discussion

3.1. UV-Vis Spectrophotometry

Rh6G, Fl, and Ag(OH)$_4^-$ concentrations were monitored with UV–Vis at their absorption maxima of 530, 490, and 270 nm, respectively (Kirschenbaum et al., 1973). During the mixing of Rh6G and Ag(OH)$_4^-$, an instantaneous decrease in concentration was observed for both species. Because of this high reaction rate, it was not possible to monitor the reaction kinetics using UV–Vis spectrophotometry. A hypsochromic shift to 490 nm was obtained for Rh6G (Fig. 1), which can be interpreted in terms of the elimination of ethyl groups responsible for the auxochromic property of the N-ethyl group (Yu et al., 2009) and the formation of N-de-ethylated species (Natarajan et al., 2011; He et al., 2009a; Li et al., 2007; Fu et al., 2005).

Fig. 2 shows the UV–Vis spectra for Fl. In this figure, the solid black line is the absorbance spectrum of a 40-ppm Fl standard solution, without Ag(OH)$_4^-$. The rest of the colored lines show the Fl degradation once Ag(III) was mixed with the dye. As noted, Fl displays its maximum absorbance at 490 nm. Since Fl has the same xanthene ring as Rh6G but without the branched groups, a preliminary interpretation of the described shift involves an early N-de-ethylation. The gradual decrease in the absorbance peak indicates the rupture of the conjugated structure (Yu et al., 2009). The Fl absorbance decrease during an 80-min experiment ended up in total discoloration (see inset). In this case, the maximum absorbance peak did not shift, which indicates that the chromophore was destroyed (i.e., the xanthene ring was attacked).

3.2. Total organic carbon (TOC)

After the oxidative discoloration of the dyes with Ag(OH)$_4^-$ was proven feasible, TOC determinations were performed to estimate
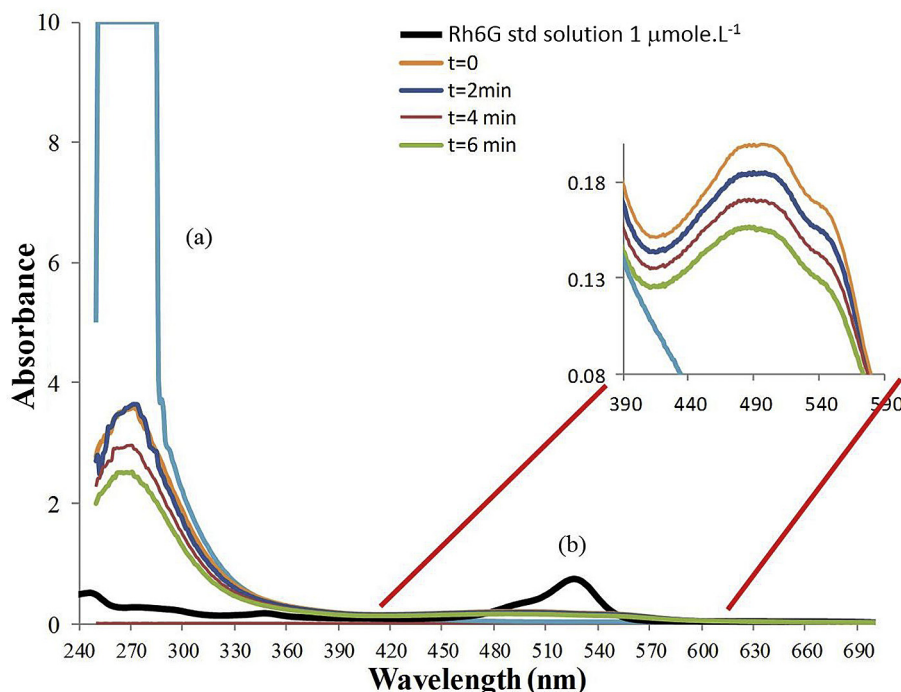

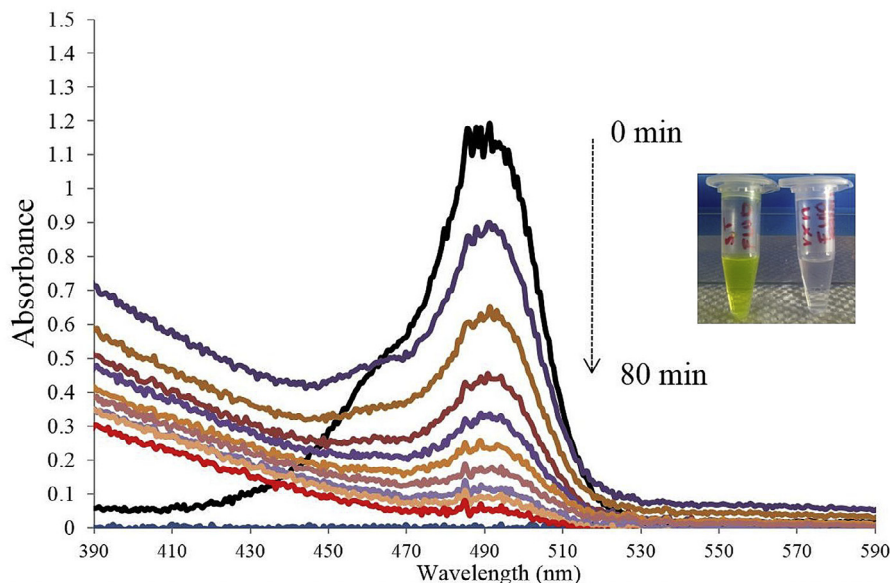**Fig. 1.** Absorbance spectra of a) Ag(OH)$_4^-$, and b) Rh6G.

Fig. 2. Absorbance spectra of fluorescein degradation.

the extent of mineralization into CO_2 as the final degradation product. Table 1 shows the results, where the organic carbon content decreased because of the reaction with $Ag(OH)_4^-$.

3.3. HPLC

The TOC results in Table 1 indicate partial mineralization. Therefore, complementary analyses are required to understand better the reaction pathway. Fig. 3 shows the HPLC results for 15-min reactions with different concentrations $Ag(OH)_4^-$ and Rh6G. Peaks are labeled according to the polarity of the samples (a < b < c < d), where a) corresponds to the Rh6G standard.

Table 1
Summary of the highest mineralization results for both dyes. The last column indicates the percentage of TOC evolved as CO_2.

Reaction	TOC (ppm)		%CO$_2$
	Initial	Final	
Ag(III)-Rh6G	11.45	7.08	**38.2**
Ag(III)-Fl	10.66	7.51	**30.5**
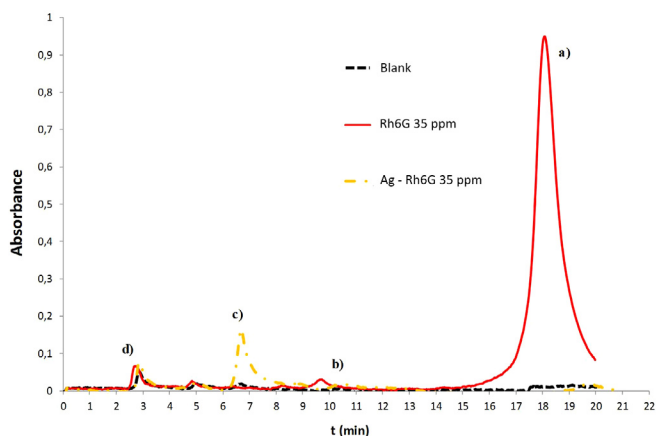
Fig. 3. Chromatograms to determine the N-de-ethylated intermediates of Rh6G.

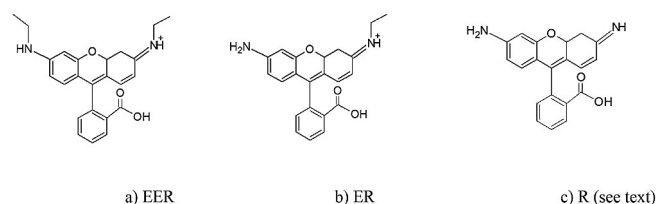| a) EER	b) ER	c) R (see text)

Fig. 4. Proposed Rh6G degradation products: a) N-ethyl-N-ethyl rhodamine, EER, b) N-ethyl rhodamine, ER and c) R.

From literature reports and previously discussed UV–Vis results, we propose that the species produced at the beginning of the reaction are those shown in Fig. 4: a) N-ethyl-N-ethyl rhodamine (EER), b) N-ethyl rhodamine (ER), and c) a compound labeled (R) in the literature (Yu et al., 2009).
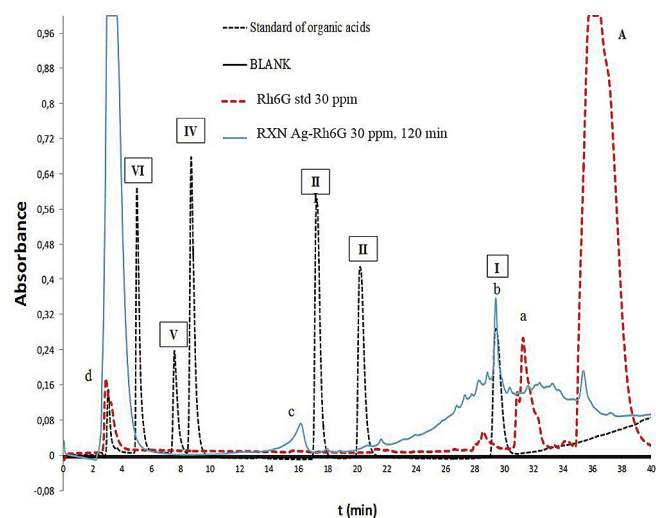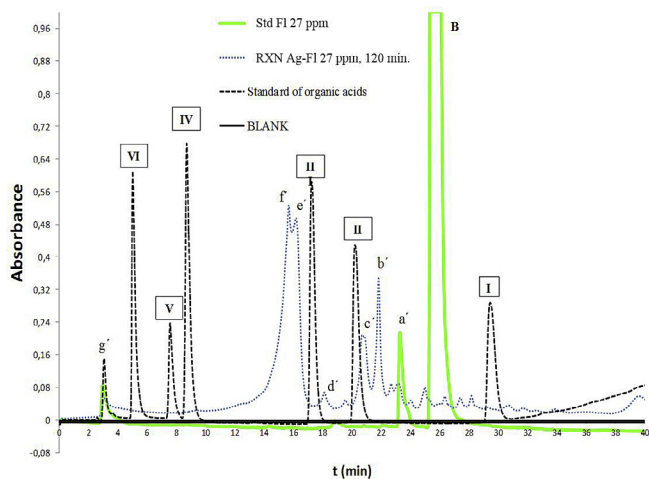
The results indicated only one intermediate (R), while the

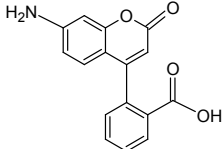**Fig. 5.** Chromatograms to determine the organic acids from the rhodamine degradation.
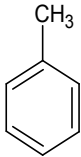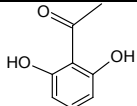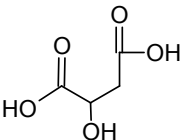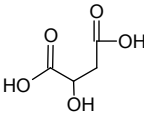
Fig. 6. Chromatograms to determine the organic acids from the fluorescein degradation.
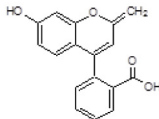
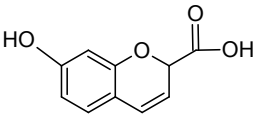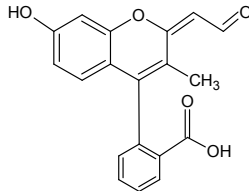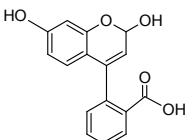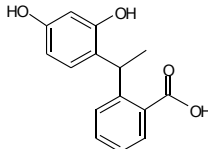rhodamine peak (a) completely disappeared. This result confirmed that most of the dye decomposed. In addition, the obtained analytes were more polar than the extracting agent (i.e., dichloromethane). Therefore, the analytes could not be efficiently recovered in the organic phase. Since peak (d) also appeared in the rhodamine standard, it did not provide supplementary information to elucidate the degradation path. To understand better the breakage of the conjugated structure into smaller analytes (e.g., organic acids), further experiments were performed using the standard addition method with ethyl acetate as the extracting agent, isocratic 45% ammonium acetate (13 mM), and 55% methanol at a detection wavelength of 250 nm.

Figures 5 and 6 show the obtained chromatograms. In both figures, the organic-acid reference standards are as follows: I, benzoic acid; II, phthalic acid; III, p-hydroxybenzoic acid; IV, gallic acid; V, succinic acid; and VI, maleic acid. In Fig. 5, peak (A) is the Rh6G standard, and peak (a) is likely an impurity in Rh6G. After 120 min of reaction with $Ag(OH)_4^-$ (i.e., the solid blue line), a 30-ppm Rh6G solution generated peak (b), which corresponds to benzoic acid (peak I, at elution time $t_e = 29$ min). Peak c) remains

Table 2
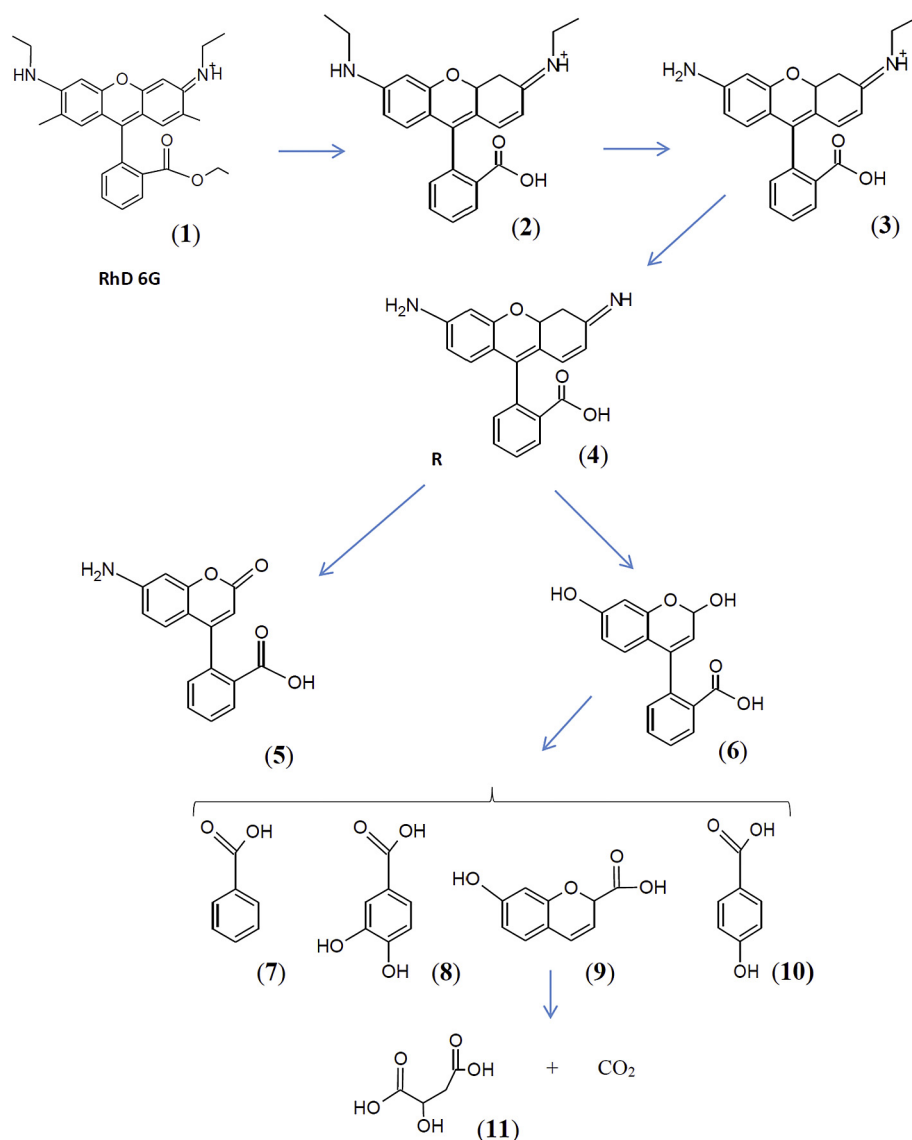Summary of the compounds involved in the degradation of both dyes.

Fig. 7. Proposed oxidative degradation pathway of Rh6G in the presence of $Ag(OH)_4^-$.

unidentified. The height of peak d) is noteworthy, and its short retention time points at small chain organic acids.

In Fig. 6, peak (B) is the Fl standard (which appears in the chromatogram of the reaction solution, a′). Likewise, after 120 min of reaction with $Ag(OH)_4^-$, a 27-ppm Fl solution generated peak b′) (unidentified, at $t_e = 22$ min), which also appeared during the decomposition of Rh6G. In addition, the Fl decomposition generated peak c′) ($t_e = 20.5$ min), which most likely corresponds to phthalic acid (II), and peaks e′) and f′) ($t_e = 16.2$ min), which most likely correspond to p-hydroxybenzoic acid (III) ($t_e = 17.2$ min) or a similar structure (note that the Rh6G decomposition also generated this peak). Finally, the peak at $t_e = 2.9$ appeared after the decompositions of both Rh6G and Fl. On a first approximation, this result can reflect the generation of maleic acid (VI); however, because this peak also appeared in the standards of both pure substances, it is difficult to speculate its exact nature. The described acids are known to be produced from the rupture of the xanthene ring (He et al., 2009a,b). Since questions remained concerning the rupture pathway, GC-MS experiments were performed next.

3.4. GC-MS

GC-MS is frequently the tool of choice for product identification, especially when assisted by the NIST 11 library. Samples identical to those in the GC-FID experiments were used. To prevent possible instrument damage caused by a high concentration input, samples were diluted 20 times with toluene. The penalty for this dilution was the loss of sensitivity for the smaller peaks.

Table 2 summarizes the compounds identified from both dyes. Previous work on the mechanism of Rh6G degradation shows that it occurs through two competing processes: N-de-ethylation with the destruction of the conjugated system, or the opening of the xanthene ring (Yu et al., 2009; He et al., 2009a,b; Li et al., 2007). From our UV–Vis, TOC, HPLC, GC-FID, and GC-MS data, we infer that both processes occurred for Rh6G and Fl during their oxidative degradation in the presence of $Ag(OH)_4^-$. The main route was the destruction of their conjugated structures followed by ring opening. This route produced organic acids, which were then mineralized to CO_2 and H_2O (He et al., 2009a). The proposed pathways are
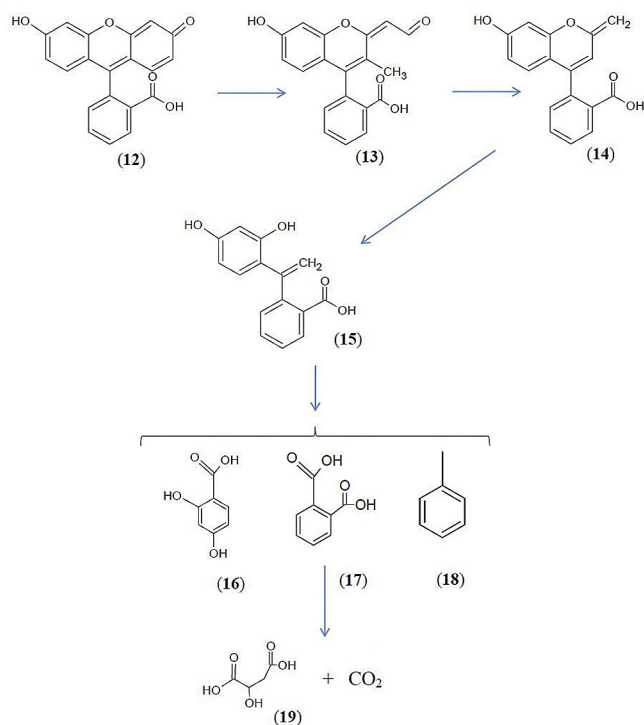
Fig. 8. Proposed oxidative degradation pathway of Fl in the presence of $Ag(OH)_4^-$.

shown in Figs. 7 and 8.

Fig. 1 shows the characteristic absorption spectra of Rh6G (at 530 nm) and of $Ag(OH)_4^-$ (at 270 nm). After mixing both solutions, a hypsochromic effect was observed (i.e., a blueshift) since the absorption maxima of Rh6G shifted to 490 nm. Such wavelength shifts have been long known to bear a definite relationship to the nature of the substituent elements (Bowden et al., 1946). Taking into account the auxochromic property of the N-ethyl group (Yu et al., 2009), this result indicates that the N-ethyl groups are eliminated, suggesting the formation of intermediate N-de-ethylated groups (Li et al., 2007, 2009; Fu et al., 2005; He et al., 2009a,b).

Since the absorption maximum of Fl is observed at 490 nm, it can be inferred that the first reaction step was the N-de-ethylation. The gradual peak decrease indicates the rupture of the conjugated structure (Yu et al., 2009). This finding is corroborated by the data in Fig. 3, where peaks b), c) and d) can be related to compounds reported earlier as part of the Rh6G N-de-ethylation (Yu et al., 2009). Therefore, the structures (2), (3) and (4) in Fig. 7, as well as (13), (14) and (15) in Fig. 8 are very likely present in the initial 15 min of reaction.

Compounds (5) and (6) were identified by GC-MS. The amino groups were oxidized by Ag(III), eventually leading to benzoic acid (7), as evidenced by HPLC using reference standards. Structures (8), (9), (10), and (11) were identified in the corresponding mass spectra. Several authors agree that the degradation process may occur by two competitive processes: a) N-de-ethylation and b) destruction of the conjugated structure or opening of the xanthene ring (He et al., 2009a,b; Yu et al., 2009; Li et al., 2007; Natarajan et al., 2011). In the case of Fl, the main products are phthalic acid (2) and p-hydroxybenzoic acid (3). Therefore, Fl undergoes an electrophilic attack that destabilizes the xanthene ring (Yu et al., 2009). From the areas under the curves, a percent degradation estimate was obtained as follows: 98.8% Rh6G degradation (i.e., 0.20 cm^2/18.0 cm^2) and 97.7% Fl degradation (i.e., 0.13 cm^2/ 5.75 cm^2).

Some advantages of the present system can be envisaged in comparison to other treatment methods. For example, in the case of degradation by chlorination, the resulting compounds may be more toxic or recalcitrant than the parent compound, or else form undesirable solids or foams (Zheng et al., 2012). In the case of supported photocatalysts, the sorption of the pollutant at the catalyst surface is required, which introduces challenges such as the requirement for strict pH control on which the extent of chemisorption or physisorption typically depends. The sorption must be sufficiently strong to provide good pollutant "adhesion" but sufficiently weak to permit light penetration and final desorption/ release after the reaction (Farida et al., 2009). If metal complexes were used to catalyze the Rh6G degradation, the choice of ligand and its speciation are crucial. For example, EDTA can hinder the Rh6G catalytic decomposition under certain circumstances and impose the requirement for further additives (e.g., hydrogen peroxide) and a stringent pH control (Li et al., 2009).

Lastly, an important aspect of the degradation of Fl is that – as for Rh6G – no precipitates were formed after the reaction with $Ag(OH)_4^-$. This fact indicates that the final silver product is Ag(I) in a soluble form, most likely as $Ag(OH)_2^-$ (Cohen and Atkinson, 1968; Zamora-Garcia et al., 2013). This result opens the possibility for developing a regenerative system, which has not been reported yet for this application.

4. Conclusions

GC/MS and HPLC analyses reveal the rupture of the conjugated chromophore xanthene ring during the oxidative degradation of rhodamine and fluorescein with $Ag(OH)_4^-$, as well as the formation of intermediate N-de-ethylated species in the case of rhodamine. The main analytical signals observed in the reaction systems (i.e., GC-FID at 5.7 min and GC-MS at MW = 134.01 m/z) indicated that $Ag(OH)_4^-$ reacted until the simplest possible organic molecules were formed, which occurred at the highest oxidant:dye molar ratio. This result is consistent with the fact that both compounds have a xanthene ring-based structure, and the present method offers a new alternative for their alkaline aqueous treatment. Despite the great structural stability of the dyes used here, they were degraded into simpler compounds, and partial mineralization was achieved. Further work with more recalcitrant and toxic compounds (e.g., pentachlorophenol) is in progress.

References

Bowden, K., Braude, E.A., Jones, E.R.H., 1946. Studies in light absorption. Part III. Auxochromic properties and the periodic system. J. Chem. Soc. 207, 948–952.

Cohen, G., Atkinson, G., 1968. The formation and characterization of the tetrahydroxyargentate (III) ion in alkaline solution. J. Electrochem. Soc. 115, 1236–1242.

Dolak, T.M., Lever, O.W., Marsh, D., Moran, I., Sutton, S., 2008. Ophthalmological preparations. In: Ullmann's Encyclopedia of Industrial Chemistry, seventh ed. Wiley, New York.

Fang-Jun, H., Jing, S., Yuan-Qiang, S., Cai-Xia, Y., Hong-Bo, T., Zong-Xiu, N., 2010. A rhodamine-based dual chemosensor for the visual detection of copper and the ratiometric fluorescent detection of vanadium. Dyes Pigm. 86, 50–55.

Farida, R., Zheng, Y., Nanayakkara, K., Chen, J., 2009. Electrochemical removal of rhodamine 6G by using RuO_2 coated Ti-DSA. Ind. Eng. Chem. Res. 48, 7466–7473.

French, J.E., 1989. Toxicology and Carcinogenesis Studies of Rhodamine 6G (C.I. Basic Red 1) (CAS No. 989-38-8) in F344/N Rats and B6C3F1 Mice (Feed Studies). U.S.

Department of Health and Human Services. Public Health Service National Institutes of Health. National Toxicology Program. Technical Report Series No. 364. Research Triangle Park, NC.

Fu, H., Pan, C., Yao, W., Zhu, Y., 2005. Visible-light-induced degradation of rhodamine B by nanosized Bi_2WO_6. J. Phys. Chem. B 109, 22432–22439.

Gear, A.R.L., 1974. Rhodamine 6G: a potent inhibitor of mitochondrial oxidative phosphorylation. J. Biol. Chem. 249, 3628–3637.

He, Z., Sun, C., Yang, S., Ding, Y., He, H., Wang, Z., 2009. Photocatalytic degradation of rhodamine B by Bi_2WO_6 with electron accepting agent under microwave irradiation: mechanism and pathway. J. Hazard. Mater. 162, 1477–1486.

He, Z., Yang, S., Ju, Y., Sun, C., 2009. Microwave photocatalytic degradation of rhodamine B using TiO_2 supported on activated carbon: mechanism implication. J. Environ. Sci. 21, 268–272.

Hochberger, J., Bayer, J., May, A., Mühldorfer, S., Maiss, J., Hahn, E.G., Ell, C., 1998. Laser lithotripsy of difficult bile duct stones: results in 60 patients using a rhodamine 6G dye laser with optical stone tissue detection system. Gut 43, 823–829.

Kirschenbaum, L., Ambrus, J., Atkinson, G., 1973. Kinetics of silver (III) complexation by periodate and tellurate ions. Inorg. Chem. 12, 2832–2837.

Lei, L., Dai, Q., 2007. High performance on the degradation of cationic Red X-GRL by wet electrocatalytic oxidation process. Ind. Eng. Chem. Res. 46, 8951–8958.

Li, J., Zhang, X., Ai, Z., Jia, F., Zhang, L., Lin, J., 2007. Efficient visible light degradation of rhodamine B by a photo-electrochemical process based on a Bi_2O_6 nanoplate film electrode. J. Phys. Chem. 111, 6832–6836.

Li, Y., Yi, Z., Zhang, J., Wu, M., Liu, W., Duan, P., 2009. Efficient degradation of rhodamine B by using ethylenediamine-$CuCl_2$ complex under alkaline conditions. J. Hazard. Mater. 171, 1172–1184.

Lide, D.R., 2007. CRC Handbook of Chemistry and Physics, 2007-2008, 88th. Edition. CRC Press, Taylor & Francis, Boca Raton, FL, pp. 8–18.

Masters, N.E., 1990. Rhodamine 6G: taming the beast. J. Forensic Identif. 40, 265–270.

Natarajan, T., Thomas, M., Bajaj, H., Tayade, R., 2011. Study on UV-LED/TiO_2 process for degradation of rhodamine B dye. Chem. Eng. J. 169, 126–134.

Peralta, J., Meas, Y., Rodríguez, F., Chapman, T., Maldonado, M., Godínez, L., 2008. Comparison of hydrogen peroxide-based processes for treating dye-containing wastewater: decolorization and destruction of Orange II azo dye in dilute solution. Dyes Pigm. 76, 656–662.

Thaler, S., Haritoglou, C., Choragiewicz, T.J., Messias, A., Baryluk, A., May, C.A., Rejdak, R., Fiedorowicz, M., Zrenner, E., Schuettauf, F., 2008. In vivo toxicity study of rhodamine 6G in the rat retina. Invest. ophth. Vis. Sci. 49, 2120–2126.

TOXNET: Toxicology Data Network, US National Library of Medicine. https://toxnet.nlm.nih.gov/cgi-bin/sis/search2/r?dbs+hsdb:@term+@DOCNO+2128. Accessed: 16 June 2017.

Wang, H., Li, Y., Xu, S., Li, Y., Zhou, C., Fei, X., Sun, L., Zhang, C., Li, Y., Yang, Q., Xu, X., 2011. Rhodamine-based highly sensitive colorimetric off-on fluorescent chemosensor for Hg^{2+} in aqueous solution and for live cell imaging. Org. Biomol. Chem. 9, 2850–2855.

Wu, K., Jane, Y., 2003. Decolorization of the textile dyes by newly isolated bacterial strains. J. Biotechnol. 101, 57–68.

Yu, K., Yang, S., He, H., Sun, C., Gu, C., Ju, Y., 2009. Visible light-driven photocatalytic degradation of rhodamine B over $NaBiO_3$: pathways and mechanism. J. Phys. Chem. 113, 10024–10032.

Zamora-Garcia, I.R., Alatorre-Ordaz, A., Ibanez, J.G., 2013. Thermodynamic and electrochemical study on the mechanism of formation of $Ag(OH)_4^-$ in alkaline media. Electrochim. Acta 111, 268–274.

Zheng, Y., Yunus, R., Nanayakkara, K., Chen, J., 2012. Electrochemical decoloration of synthetic wastewater containing rhodamine 6G: behaviors and mechanism. Ind. Eng. Chem. Res. 51, 5953–5960.